October 2025 Observing Proposal
Max Carlin, Izzy Perez, Hunter Pratt

Quasar Color Differences Against Foreground Stars

I. Introduction

Quasars, the brief phase of life for an active galactic nuclei (AGN) undergoing high accretion onto its supermassive black hole, prove to be some of most useful cosmic probes into the distant stretches of the universe. Their incredible brightness has been used to scrutinize galaxy compositions and cosmological parameters alike (Schmidt et al. 2012). Consequently, these strange objects possess different spectral energy distributions than stars and thus appear as different colors in different broadband filters (Richards et al. 2001). This peculiar difference in appearance causes quasars to appear much bluer at lower redshifts ($z < 2.5$) and redder at high redshifts (Peters et al. 2015). Accordingly, one can use these differences in color filters to differentiate between foreground stars and the accreting AGN behind them.

In an effort to quantitatively classify this difference, we intend to analyze quasars through the various color filters at our disposal. The insights gained through these observations will allow us to derive a relationship between the colors of foreground stars and their background quasars, allowing for future identification of AGN by color discrepancies.

II. Observational Design

The Sommers-Bausch Observatory (SBO) 24" telescope, Leto, possesses g', r', i' color filters to observe through. One of the key emission features of quasar spectra is their Hα emission line, which contributes a substantial amount of flux (Choi et al. 2025). To maximize our capacity to observe quasars, then, we choose to observe quasars at a redshift of $z < 0.3$ where we can capture the flux from this emission. The NASA/IPAC extragalactic database (NED) contains no shortage of objects classified as quasars at or beneath this target redshift.

The zero point magnitude in the Vega system of an object producing 1 photon/s in the red-most filter (the i' filter) is $m_{i', zeropoint, Vega} = 21.01$. According to our declination and right ascension boundaries from SBO, we can safely observe quasar targets at a magnitude much less than this zeropoint. We have found six incredibly bright, low redshift quasars with magnitude $m < 15$ (Table 1). All of these targets have desirable airmasses and altitudes from SBO (Fig. 1). Over the next month, before Nov. 21st, we have found the optimal observing times for each target by taking their maximum altitude (Table 2).

Target Name	RA	DEC	Magnitude
PG 0052+251	00 54 52.1	+25 25 39.0	14.6
B3 0133+388	01 36 32.6	+39 05 59.1	15.0
WISEA J031006.24+405654.2	03 10 06.2	+40 56 54.2	13.8
WISEA J055447.25+662043.7	05 54 47.3	+66 20 43.8	14.6
FBQS J2155-0922	21 55 01.5	-09 22 24.4	14.13
BL Lac	22 02 43.3	+42 16 40.0	14.7

Table 1. An approximate target list for our brightest targets.

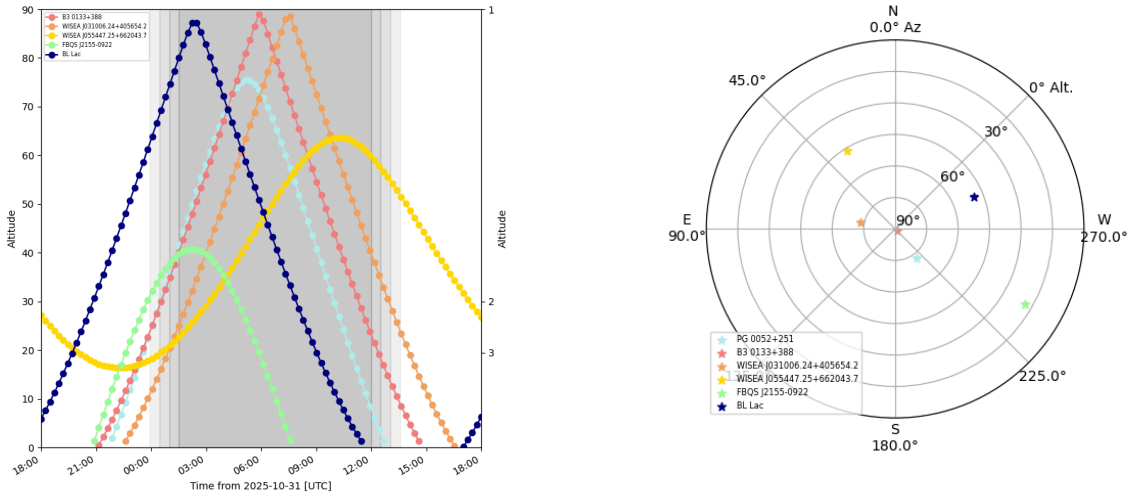

Figure 1. The airmasses and sky positions of our desired targets on 2025-10-31.

III. Observing Time

Each target will be observed through the Sloan g', r', and i' filters using the Leto 24″ telescope. Based on the typical quasar magnitudes in our sample (m ≈ 13–15), a signal-to-noise ratio (SNR) of more than, or roughly 100, can be achieved with 60–120 second exposures per filter. Including short test frames for focusing and centering, we estimate an exposure time of roughly 6 minutes per target as three 2-minute exposures.

Other telescope operations and calibrations (slewing, etc.) may add about 5 minutes per target. For a set of six quasars, this totals about 1 hour of exposure time and 30 minutes of other telescope operations, or roughly 1.5 hours of active observing.

To account for calibration frames, initial setup, and any potential weather interruptions, we propose scheduling three 2-hour observing blocks on Leto. These sessions should ideally occur around the new moon to minimize sky brightness and maximize SNR. Our group has been consistently available after 8:00 PM at least 3 times per week, which will allow us flexibility in

choosing days that have optimal viewing conditions. Any remaining time can be used to obtain repeat exposures or to add additional targets.

IV. Calibration Steps

Three methods will be utilized to calibrate our data from the 24" telescope, Leto: bias, dark, and flat-field corrections. Our bias calibration will subtract a zero second exposure. This will remove the constant baseline number of ADU that is added to all images. Our dark calibration will subtract an exposure taken with the shutter closed and of equal length and at the same temperature as the exposures we take of our targets. This will remove the thermal current effects that cause pixels to read ADU when there are no photons present. Flat-field calibration will subtract an exposure of a uniformly illuminated surface using each filter. It is important that this exposure isn't over or under saturated. This will subtract the effects of relative sensitivity between different pixels and regions on the detector.

V. Data Analysis

After calibration, we will analyze our data using the method of aperture photometry and chi-squared model fitting. This method involves defining a circular aperture around each target and each foreground star in order to find the flux emitted from each object. For each target and foreground stars we will repeat this process for each of the color filters. This will leave us with three data points of wavelength vs. flux or each target and each foreground star.

With this data we can calculate the color-indices for each object. This will involve subtracting the fluxes from each filter, and plotting this data on a single color-color graph. An example of this type of graph is shown below from the "The Fifth Data Release of the Sloan Digital Sky Survey" (Adelman-McCarthy et al. 2007). In this graph, the flux from the r' filter is subtracted from the flux from the g' filter for the y-axis, and the flux gathered from the g' filter is subtracted from u' filter in the x-axis.

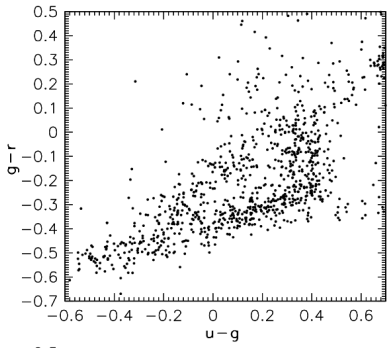

Figure 2. The g−r vs. u−g color-color diagram for objects in the sloan digital sky survey

After plotting quasars and stars on this color-color graph, we can use chi-squared model fitting to create a line of best fit for each object type. The resulting trends will allow us to determine the color differences between quasars and foreground stars, fulfilling our goal of distinguishing quasars based off of color discrepancies with foreground stars.

References

Adelman-McCarthy, J. K., Agüeros, M. A., Allam, S. S., et al. 2007, *ApJS*, 172, 634, "The Fifth Data Release of the Sloan Digital Sky Survey."

Choi, Y., Fu, Y., Im, M., Wu, X.-B., Onken, C. A., Wolf, C., et al. 2025, *arXiv:2508.06028*, "AllBRICQS: The Discovery of Luminous Quasars in the Northern Hemisphere."

Gallastegui-Aizpun, U., & Sarajedini, V. L. 2014, *MNRAS*, 444, 3078, "The ensemble optical variability of type-1 AGN in the Sloan Digital Sky Survey Data Release 7."

Peters, C. M., Richards, G. T., Myers, A. D., Strauss, M. A., Schmidt, K. B., Ivezić, Ž., Ross, N. P., et al. 2015, *ApJ*, 811, 95, "Quasar Classification Using Color and Variability."

Richards, G. T., Fan, X., Schneider, D. P., Vanden Berk, D. E., Strauss, M. A., York, D. G., Anderson, J. E., et al. 2001, *AJ*, 121, 2308, "Colors of 2625 Quasars at $0 < z < 5$ Measured in the Sloan Digital Sky Survey Photometric System."

Schmidt, K. B., Rix, H.-W., Shields, J. C., Knecht, M., Hogg, D. W., Maoz, D., & Bovy, J. 2012, *ApJ*, 744, 147, "The Color Variability of Quasars."